NASA TECHNICAL NOTE

NASA TN D-2097

SYNCHROTRON RADIATION CALCULATIONS FOR THE ARTIFICIAL RADIATION BELT

by M. P. Nakada

Goddard Space Flight Center
Greenbelt, Maryland

NATIONAL AERONAUTICS AND SPACE ADMINISTRATION • WASHINGTON, D. C. • JANUARY 1964

SYNCHROTRON RADIATION CALCULATIONS FOR THE ARTIFICIAL RADIATION BELT

By M. P. Nakada

Goddard Space Flight Center
Greenbelt, Maryland

NATIONAL AERONAUTICS AND SPACE ADMINISTRATION

For sale by the Office of Technical Services, Department of Commerce,
Washington, D.C. 20230 -- Price $0.50

SYNCHROTRON RADIATION CALCULATIONS FOR THE ARTIFICIAL RADIATION BELT

by
M. P. Nakada
Goddard Space Flight Center

SUMMARY

Calculations of synchrotron radiation from the artificial radiation belt are presented which are somewhat more detailed than those made previously. The angular distribution of the electrons and of the synchrotron radiation is considered. Omnidirectional electron fluxes given by Van Allen, Frank, and O'Brien and by Brown and Gabbe are used to derive directional fluxes. Temperatures as a function of frequency and the geomagnetic latitude at 30 Mc are calculated. The results are compared with measurements.

CONTENTS

SYNCHROTRON RADIATION CALCULATIONS FOR THE ARTIFICIAL RADIATION BELT*

by
M. P. Nakada
Goddard Space Flight Center

INTRODUCTION

Recently Peterson and Hower (Reference 1) discussed synchrotron radiation from the artificial radiation belt. They presented calculations for sky temperatures that might be expected at the geomagnetic equator from the electron flux estimates in Reference 2. Different flux estimates have been reported by Brown and Gabbe (BG) in Reference 3 and by Van Allen, Frank, and O'Brien (VFO) in Reference 4. Synchrotron radiation calculations for the BG and VFO electron fluxes are made here; these calculations include the angular distributions of the electrons and synchrotron radiation. A dipole geomagnetic field is assumed and geomagnetic latitudes are used. The fission product electron spectrum from Reference 5 is assumed.

ANGULAR DISTRIBUTION OF ELECTRONS

Figure 1 shows the electron flux maps due to BG and VFO. The dotted portions of the VFO map are extrapolations made by the author. Figure 2 shows this author's view of equatorial fluxes for BG and VFO. The marked points were

*This report has been published in essentially the same form in the *Journal of Geophysical Research*, 68(13):4079-4089, July 1963. The appendix of this report was not presented in the journal article.

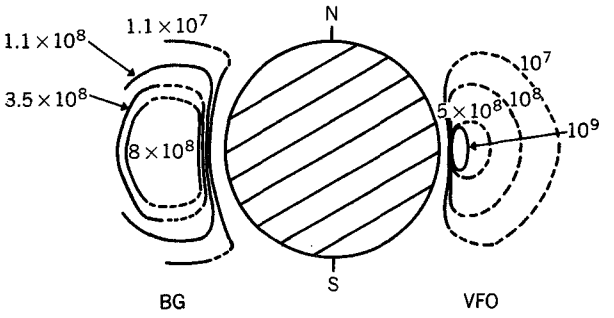

Figure 1—The BG and VFO flux maps used in the calculations. The numbers are omnidirectional fluxes in electrons/cm²-sec. The BG measurement is for 2 wk after the explosion which created the artificial belt and the VFO measurement is for +6 hr.

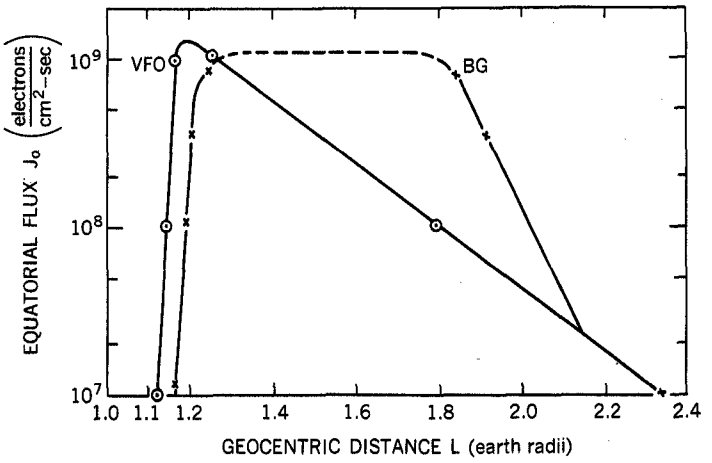

Figure 2—Omnidirectional fluxes along the geomagnetic equator.

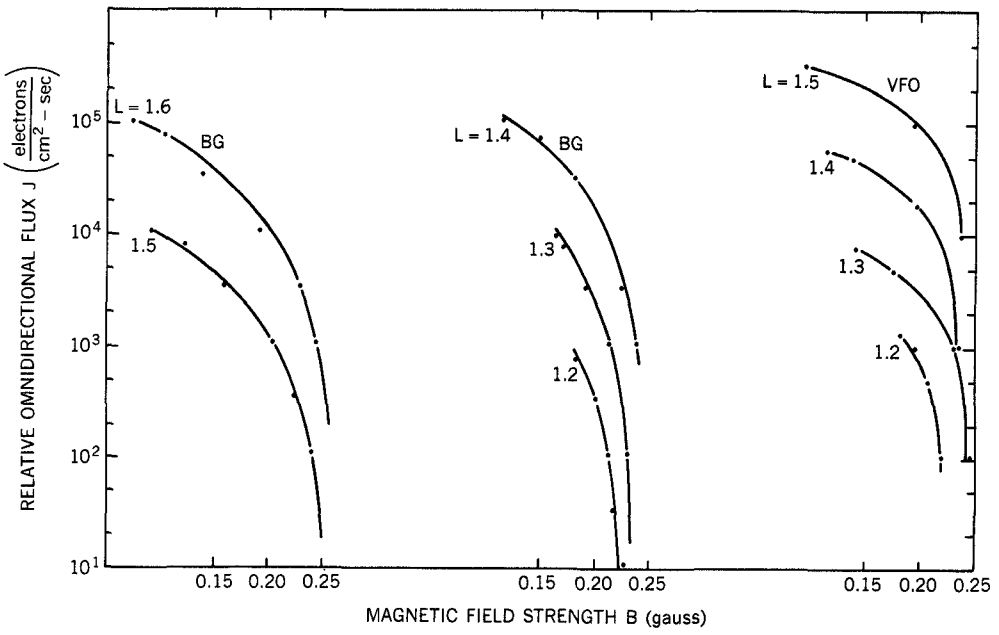

Figure 3—Relative omnidirectional fluxes vs. B along a magnetic field line. The dots indicate experimental values. The lines are the assumed analytic forms used in the calculations.

taken from BG and VFO. With these omnidirectional fluxes the directional fluxes were obtained by following the procedure in References 6 and 7. The omnidirectional flux J along a magnetic field line is plotted as a function of the magnetic field strength, as in Figure 3. Because of the scarcity of experimental points, analytic forms of J were used to fit the plotted points. Figure 3 shows a comparison between J values from Figures 1 and 2 and J values used in the calculations. The analytic form used for BG is proportional to $(B - B_{max})^2$ and for VFO it is proportional to $B - B_{max}$, where B is the magnetic field for J and B_{max} is the field when J is small. The equatorial omnidirectional flux J_0 and B_{max} are then sufficient to determine J along a field line. Equation 6 from Reference 7 has been used to determine the equatorial directional flux from the omnidirectional flux. Liouville's theorem and the equation of

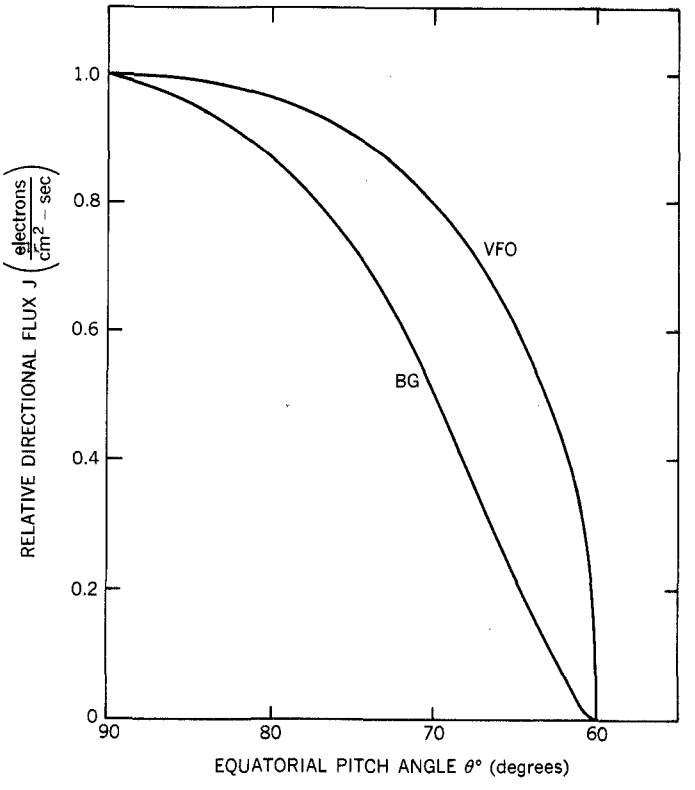

Figure 4—Relative shapes of directional flux curves for the BG and VFO flux estimates.

motion of the electrons, $\sin^2 \theta = (B/B_0) \sin^2 \theta_0$, have been used to determine the directional fluxes away from the equator; θ and B are the pitch angle and magnetic field respectively; the subscript zero refers to equatorial values. Figure 4 shows the equatorial directional fluxes as a function of pitch angle.

The half-angles of electron angular distributions at the equator have been plotted in Figure 5 for later comparison with the width of synchrotron radiation. The half-angle is the pitch angle measured from the normal to the field line to where the directional flux is half the directional flux at 90 degrees to the field. Figure 6 shows variations in pitch angles with geomagnetic latitude.

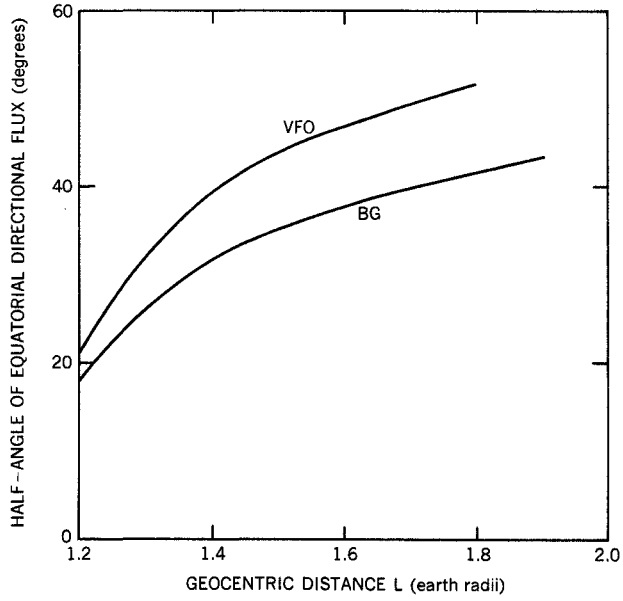

Figure 5—Half-width of equatorial directional fluxes.

ANGULAR DISTRIBUTION OF SYNCHROTRON RADIATION

The power radiated in the n^{th} harmonic of the cyclotron frequency into a unit solid angle at angle ψ with the instantaneous orbital plane has been given by Schwinger (Reference 8). The ψ-dependent part is given by

$$\left[J_n'(n\beta \cos \psi)\right]^2 + \frac{\tan^2 \psi}{\beta^2} \left[J_n (n\beta \cos \psi)\right]^2,$$

where J_n' and J_n are Bessel functions and β is the ratio of the velocity of the electron to the velocity of light. The angular distribution relative to $\psi = 0$ has been evaluated. Angles at which the power radiated is half of the $\psi = 0$ values ($\psi_{1/2}$) are plotted in Figure 7 for a number of electron energies. The abscissa is $n(1 - \beta^2)^{1/2}$, which is equal to $\nu/(2.8 B \sin \theta)$, where ν is the frequency in Mc, B is the magnetic field in gauss, and θ is the pitch angle of the electron relative to B. These results show that the angular distribution has a rather small dependence on electron energy for a given value of $\nu/(B \sin \theta)$. At 30 Mc for B = 0.2 gauss, a

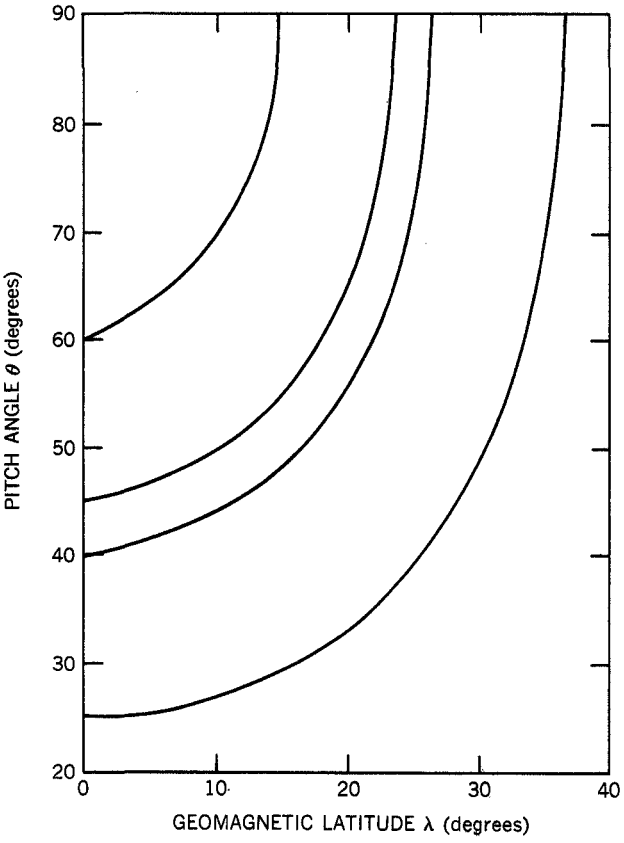

Figure 6—Variation of pitch angle with geomagnetic latitude.

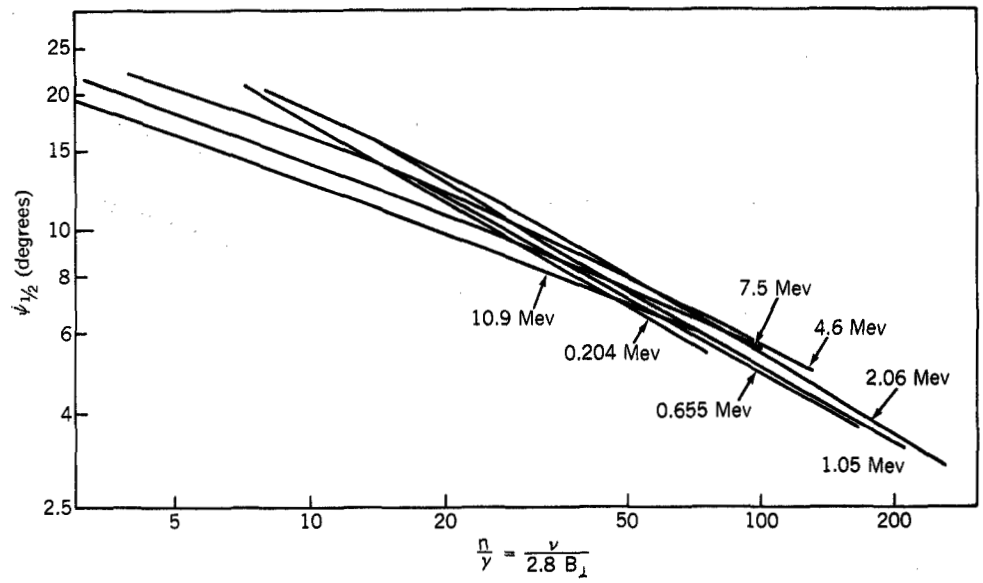

Figure 7—Half-width of the synchrotron radiation pattern.

value near the earth, $\psi_{1/2}$ is about 7.8 degrees. At 50 Mc for the same B value, $\psi_{1/2}$ is about 6.0 degrees. For smaller values of B, $\psi_{1/2}$ is, of course, narrower. Thus, the angular distribution of the synchrotron radiation is usually narrower than that of the electron angular distribution for the frequencies and magnetic fields discussed in this report.

CALCULATION OF TEMPERATURES

The brightness along a line of sight is given by $\int (dP/d\Omega)\ dR$ where $dP/d\Omega$ is the power emitted per unit volume along the line of sight per steradian; the integration is along the line of sight R. Since the synchrotron radiation pattern is usually narrower than that of the electrons, the following approximation has been used to find the brightness, b:

$$b(\nu) = \int P(\nu,\ B \sin\theta)\ \frac{j(\theta)}{\beta c}\ dR \quad . \tag{1}$$

$P(\nu,\ B \sin\theta)$ is the total power emitted per unit frequency at frequency ν for an electron moving toward the observer. This electron has a pitch angle θ with the magnetic field B; $j(\theta)$ is the directional flux of fission product decay electrons; and

$$P(\nu,\ B \sin\theta) = \int P(E,\ \nu,\ B \sin\theta)\ N(E)\ dE \quad ,$$

where E is the electron energy, N(E) is the normalized electron spectrum, and $P(E,\ \nu,\ B \sin\theta)$ is the total power emitted per unit frequency at ν and $B \sin\theta$ for an electron with energy E.

Although Equation 1 is an approximation, errors introduced through its use are small for electron and radiation pattern widths considered in this report. For an exact $dP/d\Omega$ the radiation pattern

(slightly different at each angle and electron energy) should be folded into the electron angular distribution, and the result of this fold along the line of sight should be used. If the electron and radiation distributions are assumed to be gaussian, the result of the fold will give a pattern whose width is given by the square root of the sum of the squares of the assumed gaussians. For most distributions considered in this report, the resulting gaussian is only a few percent broader than an appropriate electron distribution gaussian. Since both the electron and radiation distributions fall off more rapidly than appropriate gaussians, the true fold should be narrower than the result of folding the gaussians. In order that the effect of folded patterns that are broader than the electron pattern might be assessed, calculations have been made by increasing the electron width to exceed the result of the fold at all points. The calculated temperatures indicate that errors introduced through the use of Equation 1 are small.

The relativistic formula for $P(\nu, B \sin\theta, E)$ is (Reference 9)

$$P(\nu, B \sin\theta, E) = C B \sin\theta \int_{\alpha}^{\infty} K_{5/3}(\eta) d\eta \quad , \tag{2}$$

where C is a constant equal to 2.34×10^{-22} ergs/sec-cycle/sec,

$$\alpha = \frac{\nu(Mc)}{4.2\gamma^2 B \sin\theta} \quad ,$$

$$\gamma = \left(1 - \beta^2\right)^{-1/2} \quad ,$$

and $K_{5/3}$ is a Bessel function. This formula gives upper limit values. $F(\alpha) = \alpha \int_{\alpha}^{\infty} K_{5/3}(\eta)\, d\eta$ is plotted in Figure 8. Corresponding values for the nonrelativistic formula (Reference 8, formula III.28) are also shown in Figure 8. These results indicate that, where radiation by electrons is efficient the relativistic formula is a satisfactory approximation but an upper limit.

Equation 1 with $\beta = 1$ has been used to evaluate sky brightness. The Rayleigh-Jeans approximation to the Plank radiation formula was used to convert brightness to temperature T; $b = 2kT/\lambda^2$, where k is Boltzmann's constant and λ is the wavelength. Figure 9 shows sky temperatures at 30 Mc for the BG flux for an observer at 20°N geomagnetic latitude.

Figure 10 shows calculated temperatures as a function of frequency for the BG and VFO fluxes for an observer at the geomagnetic equator looking vertically. At the equator, the temperatures that are calculated for

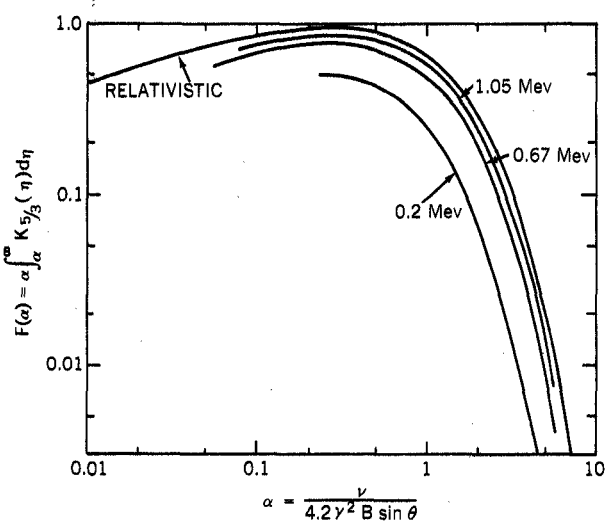

Figure 8—Comparison between relativistic and nonrelativistic synchrotron radiation-power formulas.

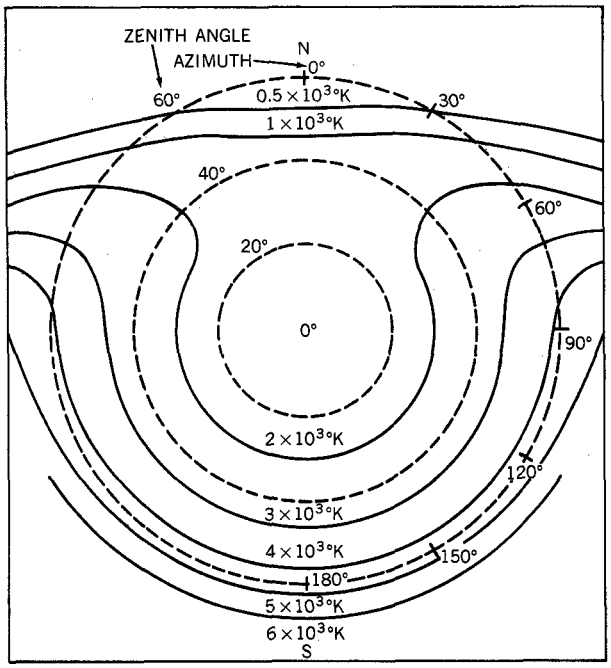

Figure 9—Sky brightness map due to the artificial radiation belt. Sky temperatures are at 30 Mc for 20° N geomagnetic latitude and BG flux. The solid lines are isophots.

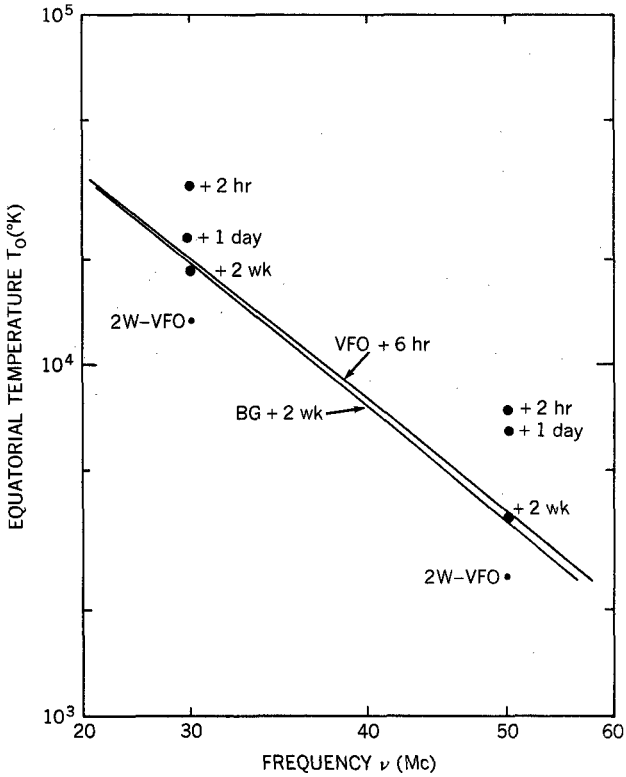

Figure 10—Comparison between calculated and observed sky temperatures at the geomagnetic equator.

a narrow beam antenna and a $\cos^2 Z$ antenna are very nearly the same (Z is the zenith angle).

Despite the time difference for the two flux estimates (VFO at 6 hr and BG at 2 wk after the detonation) the results are nearly the same. The VFO values tend to be higher than BG at higher frequencies. This is to be expected since VFO fluxes are higher at lower altitudes and higher frequencies show a greater decrease in radiation with altitude (Reference 1).

The experimental points in Figure 10 are taken from measurements by Ochs, Farley, et al. (Reference 10). Adjacent to the points are the times after the explosion. The pre-explosion background which they used, obtained from a sky survey, was 5200°K at 50 Mc at 0600 local time. The 30 Mc background temperature of 15,000°K at this time was obtained from their ratio of 30 to 50 Mc temperatures before the explosion. Temperatures have also been calculated at 30 and 50 Mc for an estimated flux for VFO at 2 weeks after the detonation. The BG equatorial flux was used for $L = 1.16$ to 1.28; the VFO flux was used for $L = 1.28$ to 2.3. The BG angular distribution has been used. Temperatures for this flux estimate are labeled 2W-VFO in Figure 10.

The calculated changes in temperatures with geomagnetic latitude at 30 Mc, for observers looking vertically, with $\cos^2 Z$ antennas, are plotted in Figures 11 and 12 for the BG and VFO flux estimates. The experimental measurements from Dyce and Horowitz (Reference 11) are temperatures normalized to the diurnal minimum before the explosion for what is approximately a $\cos^2 Z$

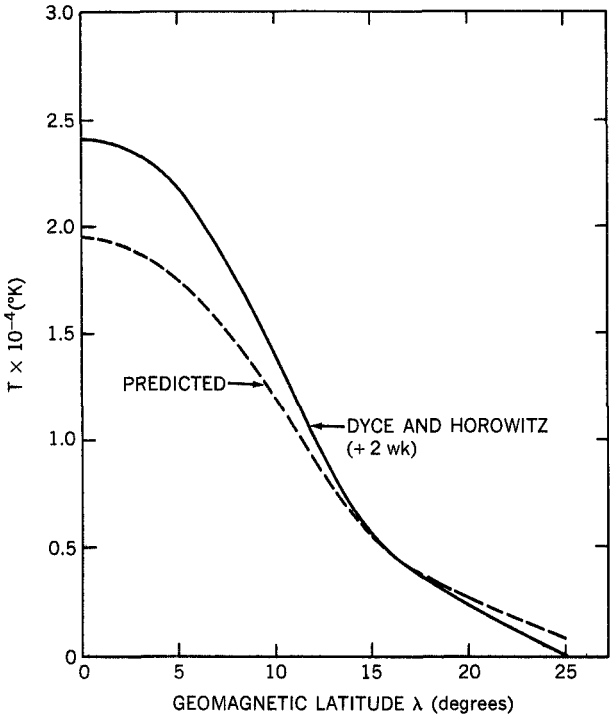

Figure 11—The dashed curve shows predicted sky temperatures for vertically directed antennas with a $\cos^2 Z$ pattern for the BG flux estimates at +2 wk and different geomagnetic latitudes. The solid curve is the experimental curve from Reference 11; this curve has been renormalized and a decay has been included.

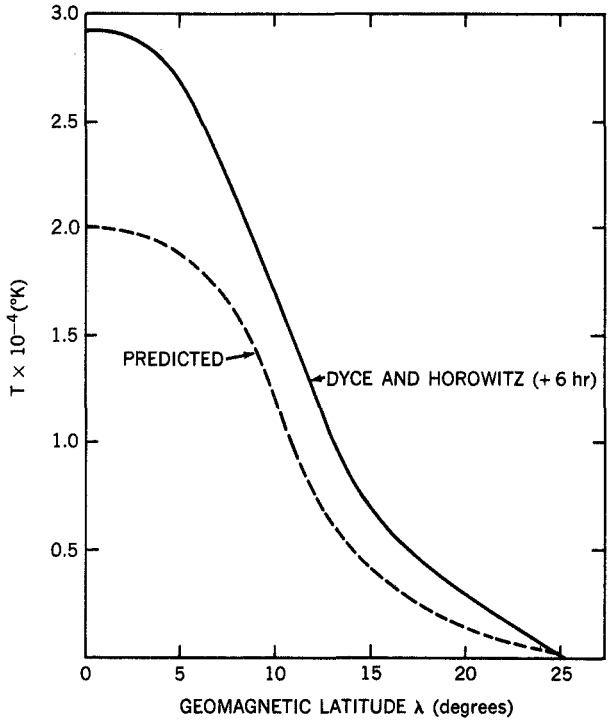

Figure 12—The dashed curve shows predicted sky temperatures at +6 hr for vertically directed antennas with a $\cos^2 Z$ pattern for the VFO flux estimate at different geomagnetic latitudes. The solid curve is the renormalized experimental curve from Reference 11.

antenna. Dyce and Horowitz used 10^4 °K for this minimum temperature. This seems rather low for their antennas since interpolation of the Turtle, Pugh, et al. results at 26.3 and 38 Mc gives a minimum temperature of 10^4 °K at 30 Mc for an antenna with a 15 degree right ascension by 44 degree declination antenna (Reference 12). Estimates for a $\cos^2 Z$ antenna, using the absolute temperature maps due to Turtle, Pugh, et al. (Reference 12) and Steiger and Warwick (Reference 13), indicate that the normalization temperature at 30 Mc for the diurnal minimum was probably near 1.5×10^4 °K. The latitude distribution plotted in Figures 11 and 12 uses this estimated normalization temperature. For the BG comparison a $\left[1 + (t/t_0)\right]^{-1}$ decay with $t = 60$ days has been used at all latitudes, although +2 wk measurements at the geomagnetic equator are in agreement with calculated temperatures (see Figure 10).

DISCUSSION

Calculated equatorial temperatures seem to indicate that the VFO flux may be inadequate to explain measured temperatures at +6 hr. The BG flux appears to give satisfactory agreement with observations at +2 wk.

The latitude distribution is more sensitive to fluxes at larger L values. VFO flux shows greater temperature deviations from observations at higher latitudes. Whether the BG flux estimate is in agreement with observations depends on measurements of absolute temperatures for the antennas used and on measurements at +2 wk.

The largest difference between the two flux estimates is for $L > 1.28$. If a fission spectrum is assumed for the difference between the two flux estimates ($L > 1.28$), the calculated equatorial temperature for this difference flux at 50 Mc is 941°K. The BG angular distribution was used in this calculation which is for a narrow beam antenna pointed vertically. This temperature may be compared with the minimum detectable temperature of about 40°K at 50 Mc (Reference 10) obtained with polarization techniques. Ochs, Farley, et al. attempted to observe synchrotron radiation from the natural radiation belt immediately prior to the detonation, but detected no positive signal (Reference 10). From this it may be inferred that if the difference between the two flux estimates was natural but had a spectrum similar to that of fission product decay electrons, then it should have been detectable. Electrons with energy less than 2 Mev do not contribute appreciably to 50 Mc radiation for this difference flux.

Brown and Gabbe were unable to distinguish any spectral difference between regions where the fission spectrum was highly probable and the difference-flux regions (Reference 3). However, their detector was not sensitive enough to distinguish between spectra where the portions greater than 2 Mev may be very different.

Van Allen, Frank, and O'Brien found from their Injun I (1961 $o2$) data that the artificial belt spectrum is considerably *harder* than the natural one at $L \approx 4$ but whether this hardening extends to equatorial regions in the same way is not known. Explorer XII (1961 $\upsilon 1$) traversed a region of the artificial belt and had a detector sensitive to electrons with energy greater than 1.6 Mev, but detailed studies of its data have not been published. Perhaps the Explorer XII results, spectral and decay studies from Explorers XIV (1962 $\beta\gamma 1$) and XV (1962 $\beta\lambda 1$), and Telstar I (1962 $\alpha\epsilon 1$) results, in conjunction with the negative polarization results of synchrotron radiation prior to the explosion, will shed light on what fraction of the BG observations was natural.

CONCLUSIONS

Angular distributions of electrons have been used that are consistent with published omnidirectional flux maps of BG and VFO. The angular distribution of synchrotron radiation has been found to be considerably narrower than that of the electrons for most situations. The fold of the synchrotron radiation pattern onto the electron angular distribution should have a shape slightly wider than that of the electrons.

Since the electron distribution has been used to represent the result of the folded radiation and electron distribution, calculations have been made with electron distributions broader than the result of the fold at all locations. The deviations due to this broadening were found to be small.

Although the relativistic radiation formula tends to give upper limit results, evaluation of the nonrelativistic formula shows that the relativistic approximation is quite adequate even at frequencies

lower than those considered here. For the assumed magnetic fields, electron spectrum, and fluxes, these calculations have been estimated to have an uncertainty of about 10 percent.

The VFO flux estimate has been found inadequate to explain the observed temperature at the equator and at higher latitudes. The adequacy of the BG estimate will depend on absolute calibration of antennas and on later results, although present estimates of absolute temperatures for the antennas indicate good agreement between measured and calculated temperatures. Calculated temperatures for the difference between the BG and VFO fluxes for $L > 1.28$ set limits on electron spectra in the natural radiation belt prior to the explosion. This result, in conjunction with satellite measurements, may determine what fraction of the BG flux estimate was natural.

Appendix A contains calculations on the synchrotron radiation which might be expected at lower frequencies.

ACKNOWLEDGMENTS

I gratefully acknowledge the work of Tom Michels who made the calculations involving Bessel functions, and Robert Baxter who set up the code for the detailed temperature calculation.

REFERENCES

1. Peterson, A. M., and Hower, G. L., "Synchrotron Radiation from High-Energy Electrons," *J. Geophys. Res.* 68(3):723-734, February 1, 1963.

2. Hess, W. N., "The Artificial Radiation Belt Made on July 9, 1962," NASA Technical Note D-1687, April 1963; also *J. Geophys. Res.* 68(3):667-683, February 1, 1963.

3. Brown, W. L., and Gabbe, J. D., "The Electron Distribution in the Earth's Radiation Belts During July 1962 as Measured by Telstar," *J. Geophys. Res.* 68(3):607-618, February 1963.

4. Van Allen, J. A., Frank, L. A., and O'Brien, B. J., "Satellite Observations of the Artificial Radiation Belt of July 1962," *J. Geophys. Res.* 68(3):619-627, February 1, 1963.

5. Carter, R. E., Reines, F., et al., "Free Antineutrino Absorption Cross Section. II. Expected Cross Section from Measurements of Fission Fragment Electron Spectrum," *Phys. Rev.* 113(1):280-286, January 1, 1959.

6. Ray, E. C., "On the Theory of Protons Trapped in the Earth's Magnetic Field," *J. Geophys. Res.* 65(9):1125-1134, April 1960.

7. Farley, T. A., and Sanders, N. L., "Pitch Angle Distributions and Mirror Point Densities in the Outer Radiation Zone," *J. Geophys. Res.* 67(6):2159-2168, June 1962.

8. Schwinger, J., "On the Classical Radiation of Accelerated Electrons," *Phys. Rev.* 75(12):1912-1925, June 15, 1949.

9. Westfold, K. C., "The Polarization of Synchrotron Radiation," *Astrophys. J.* 130(1):241-258, July 1959.

10. Ochs, G. R., Farley, D. T., Jr., et al., "Observations of Synchrotron Radio Noise at the Magnetic Equator Following the High-Altitude Nuclear Explosion of July 9, 1962," *J. Geophys. Res.* 68(3):701-711, February 1, 1963.

11. Dyce, R. B., and Horowitz, S., "Measurements of Synchrotron Radiation at Central Pacific Sites," *J. Geophys. Res.* 68(3):713-721, February 1, 1963.

12. Turtle, A. J., Pugh, J. F., et al., "The Spectrum of the Galactic Radio Emission. I. Observations of Low Resolving Power," *Mon. Not. Roy. Astronom. Soc.* 124(4):297-312, 1962.

13. Steiger, W. R., and Warwick, J. W., "Observations of Cosmic Radio Noise at 18 Mc/s in Hawaii," *J. Geophys. Res.* 66(1):57-66, January 1961.

Appendix A

Synchrotron Radiation at Low Frequencies

Since there is some interest in the amount of synchrotron radiation produced by the artificial radiation belt at lower frequencies, calculations have been extended to 1 Mc. The procedure already given has been followed except for two changes. The first change was to take into account the wider resultant of the fold of the radiation pattern onto the electron distribution. This was done by artificially broadening the electron distribution to a width that was comparable with that of the folded electron and radiation distribution. This is not entirely satisfactory. However, the final results were not sensitive to variations in broadening near the appropriate final width. The second change was a correction to the results, necessary because of the use of the relativistic formula for the total power. In making this correction, the contribution of energy intervals in the electron spectrum to the total power was evaluated (see the equation after Equation 1). Then Figure 2 was used in finding the factor for reducing the contribution of the energy intervals. Figure A1 shows predicted temperatures for an equatorial observer with a $\cos^2 Z$ antenna for the BG flux estimate (July 23, 1962). Ionosphere absorption has been neglected.

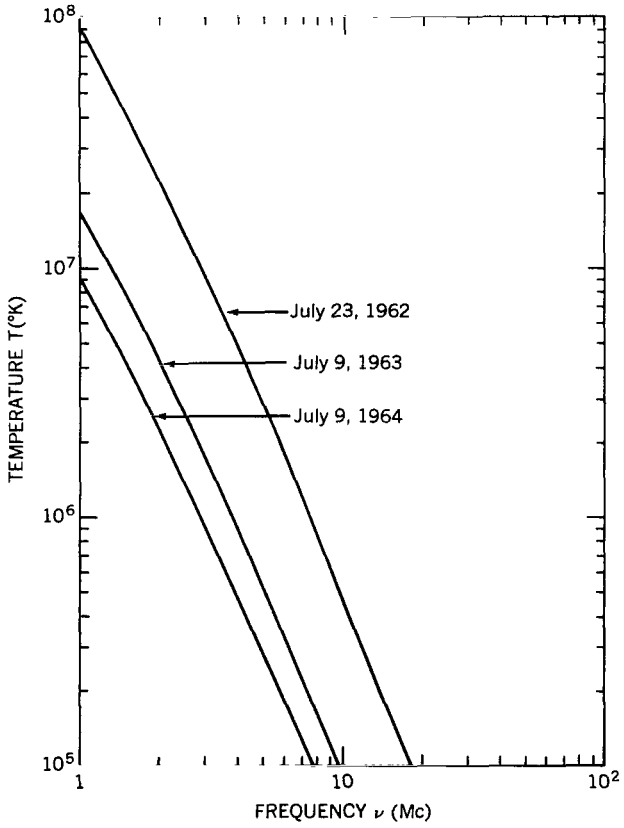

Figure A1—Temperature vs. frequency for an observer at the geomagnetic equator with a $\cos^2 Z$ antenna.

Both synchrotron radiation and satellite measurements show considerable decay in the artificial radiation belt. At 30 Mc at the geomagnetic equator the decay appears to follow a

$(1 + t/t_0)^{-1}$ law with t_0 = 60 days.* At lower frequencies the decay should be comparable since the energetic electrons which give synchrotron radiation at 30 Mc also produce an appreciable fraction of the lower frequency radiation. Less than 17 percent of the 1 Mc radiation is produced by fission product electrons with less than 0.5 Mev energy. Estimates using this decay law are also shown in Figure A1 (July 9, 1963, and July 9, 1964).

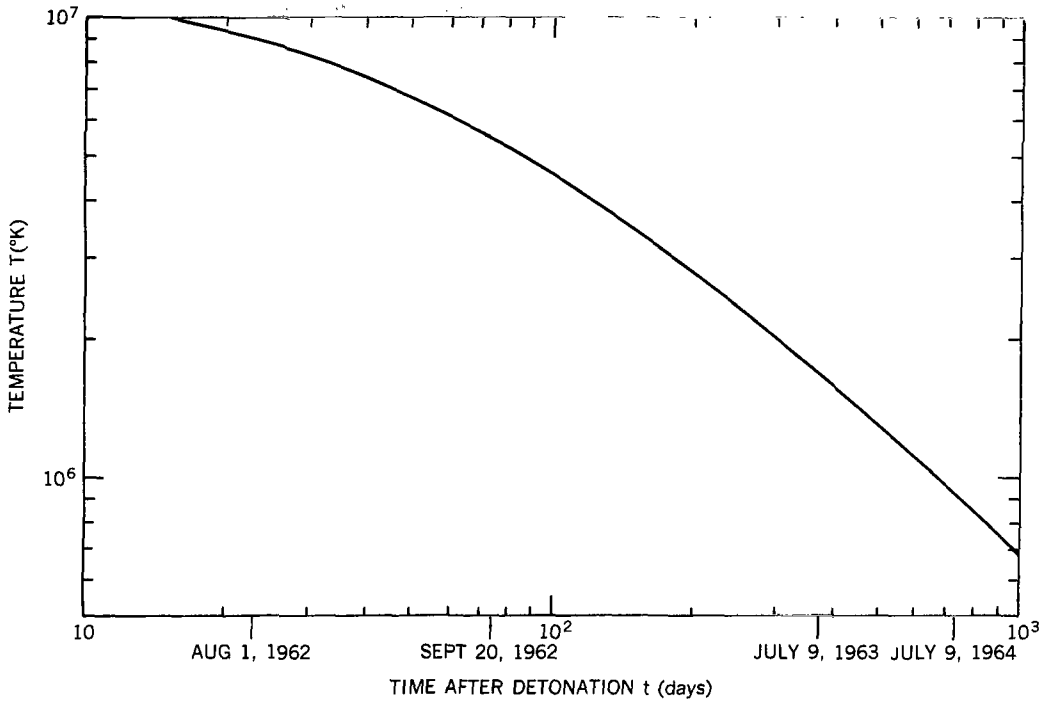

Figure A2—Temperature vs. time at 52°N geomagnetic latitude, L = 1.27, and ν = 1 Mc.

A rocket was flown to measure low frequency galactic radio noise. Its coordinates at apogee were approximately 1.27 earth radii from the center of an assumed dipole and 52°N geomagnetic latitude. Calculations have been made at 1 Mc for this apogee location (Figure A2). Since the rocket was spinning, a 4π steradian antenna and a perfectly reflecting ionosphere were assumed.

*Ochs, G. R., Farley, D. T., Jr., et al. "Observations of Synchrotron Radio Noise at the Magnetic Equator Following the High-Altitude Nuclear Explosion of July 9, 1962," *J. Geophys. Res.* 68(3):701-711, February 1963.